Novel Structural Motifs in Oxidized Graphene

H. J. Xiang,[1] Su-Huai Wei,[2] and X. G. Gong[1]

[1]*Key Laboratory for Computational Physical Sciences, Ministry of Education, P. R. China, and Department of Physics, Fudan University, Shanghai 200433, P. R. China*

[2]*National Renewable Energy Laboratory, Golden, Colorado 80401, USA*

(Dated: December 31, 2009)

Abstract

The structural and electronic properties of oxidized graphene are investigated on the basis of the genetic algorithm and density functional theory calculations. We find two new low energy semiconducting phases of the fully oxidized graphene (C_1O). In one phase, there is parallel epoxy pair chains running along the zigzag direction. In contrast, the ground state phase with a slightly lower energy and a much larger band gap contains epoxy groups in three different ways: normal epoxy, unzipped epoxy, and epoxy pair. For partially oxidized graphene, a phase separation between bare graphene and fully oxidized graphene is predicted.

PACS numbers: 61.48.Gh,73.61.Wp,71.20.-b,73.22.-f

Graphene, a single layer of honeycomb carbon lattice, exhibits many exotic behaviors, ranging from the anomalous quantum Hall effect [1–3] and Klein paradox [4] to coherent transport [5]. Because of its exceptional electrical, mechanical, and thermal properties, graphene holds great promise for potential applications in many technological fields such as nanoelectronics, sensors, nanocomposites, batteries, supercapacitors and hydrogen storage [6]. Nevertheless, several of these applications are still not feasible because the large-scale production of pure graphene sheets remains challenging. Currently, graphene oxide (GO) is of particular interest since chemical reduction of GO has been demonstrated as a promising solution based route for mass production of graphene [7–11]. In addition, GO shows promise for use in several technological applications such as polymer composite [12], dielectric layers in nanoscale electronic devices, and the active region of chemical sensors.

GO, which was first prepared by Brodie [13] in 1859, consists of oxidized graphene layers with the hexagonal graphene topology [14]. Although it is now widely accepted that GO bears hydroxyl and epoxide functional groups on its basal plane [15], as confirmed by a recent high-resolution solid-state ^{13}C-NMR measurement [16], the complete structure of GO has remained elusive because of the pseudo-random chemical functionalization of each layer, as well as variations in exact composition.

Several first-principles studies [17–20] have been performed to investigate the structure and energetics of epoxide and hydroxyl groups on single-layer graphene. In those calculations, some possible structures were manually selected and examined in order to obtain a good structural model for GO. In this Letter, we adopt the genetic algorithm (GA) in combination with density functional theory (DFT) to search the global minimum structures of oxidized graphene with different oxidation levels. As a first step, we consider only the arrangement of epoxide groups on single-layer graphene. We find two new graphene based low energy structures of C_1O. In both structures, there are epoxy pairs and some carbon-carbon σ bonds are broken. However, the two structures of C_1O have dramatically different electronic properties: one has a much larger band gap than the other, and the low band gap structure has a conduction band minimum (CBM) which is even lower than the Dirac point of graphene. We also show that for C_xO with low oxygen (high x) concentration, a phase separation between bare graphene and the low energy structures of C_1O will take place in the ground state. In addition, the electronic structure of C_xO will depend on which low energy structure is present in the system. Our results are directly relevant to the oxidation

of graphene in O_2 atmosphere [21] or oxygen plasma [22]. They also have important implications for understanding the structural and electronic properties of GO made by mineral acid attack.

We perform global structure searches based on the GA. The GA has been successfully applied to find the ground state (GS) structure of clusters [23], alloys [24], and crystals [25]. In this work, we consider all possible inequivalent (6 in total) graphene supercells up to 8 carbon per cell. For each graphene supercell, we perform several GA simulations to confirm the obtained GS structure. Here, the oxygen atoms can only occupy the bridge sites of both sides of the graphene plane. It can be easily seen that the number of possible oxygen positions on both sides of the graphene is thrice the number of carbon atoms. However, two oxygen atoms at nearest bridge sites is very unstable due to the short O-O distances (about 1.2 Å), thus the lowest C/O ratio for a possible stable structure is 1. Different oxygen concentrations are simulated: C/O= 1, C/O= 2, C/O= 3 and C/O= 4. For a given graphene supercell and C/O ratio, we first randomly generate tens (e.g., 16) of structures of C_xO. Then we fully optimize the internal coordinations and cell of structure. To generate new population, we perform the cut and splice crossover operator [23, 25] on parents chosen through the tournament selection. In an attempt to avoid stagnation and to maintain population diversity, a mutation operation in which some of the oxygen atoms can hop to other empty bridge sides is introduced. In this study, we use DFT to calculate the energies and relax the structures. Our first principles DFT calculations are performed on the basis of the projector augmented wave method [26] encoded in the Vienna ab initio simulation package [27] using the local density approximation (LDA) and the plane-wave cutoff energy of 500 eV.

To characterize the stability of oxidized graphene structures, we define the formation energy or oxygen absorption energy as:

$$E_f = E(C_xO) - x\mu_C - \mu_O \tag{1}$$

where μ_C is set to be the energy of graphene per carbon atom, and $\mu_O = 1/2E(O_2)$ [$E(O_2)$ is the energy of an isolated triplet oxygen molecule]. It should be noted that the relative stability between various structures of oxidized graphene does not depend on the particular choice of the oxygen chemical potential (μ_O). Our GA simulations reveal two low energy structures of C_1O, as shown in Fig. 1. In both structures, each of the carbon atoms bonds

with two neighbor carbon atoms and two O atoms, thus there is no sp^2 carbon. The structure shown in Fig. 1(b) is rather simple: There are epoxy pair chains along the zigzag direction which are parallel to each other. We will refer to this model as the epoxy pair model (D_{2h} symmetry) hereafter. The formation of an isolated epoxy pair was suggested in a theoretical study on the graphene oxidative process [28]. It was also shown that an isolated epoxy pair is less stable than a carbonyl pair [28]. However, in the fully oxidized graphene case, we find that the epoxy pair chain is more stable than the carbonyl pair chain by about 0.84 eV per pair. The lowest energy structure (C_{2v} symmetry) [Fig. 1(a)] of C_1O has a lower energy than the epoxy pair model by only 60 meV/O. The small energy difference suggests that both phases might coexist at finite temperature. In the lowest energy structure, there are isolated six-membered carbon rings, which are connected to the neighboring six-membered carbon rings through two epoxy pairs and four unzipped epoxy groups. For each six-membered carbon ring, there are two normal epoxy groups. Therefore, we term this complex structure as the mix model. One can obtain the epoxy pair model from the mix model by moving the unzipped epoxy groups on top of the normal epoxy groups.

The low energy structures of oxidized graphene with C/O= 2 and C/O= 4 are displayed in Fig. 2. Among all C_2O structures with no more than eight C atoms per cell, the lowest energy structure has two neighboring epoxy pair chains and half of the carbon atoms remain sp^2 hybridized. For comparison, we also show the C_2O structure predicted by Yan *et al.* [19] in which no carbon-carbon bond is broken and all carbon atoms are sp^3 hybridized. Test calculations show that our identified new structure is more stable by almost 0.40 eV/O than Yan's structure with normal epoxy groups. For C_4O, we find that oxygen atoms tend to form isolated chains. In the lowest energy structure, the graphene is unzipped by an oxygen chain and the normal epoxy groups are connected with the unzipped epoxy groups. In another metastable structure, there is an isolated epoxy pair chain. The isolated epoxy pair chain structure is less stable than the lowest energy structure by only 30 meV/O. The isolated epoxy pair chain structure is found to be the lowest energy structure of C_3O with no more than six carbon atoms.

The calculated formation energies of the above discussed lowest energy structures are about -1.2 eV/O, -0.9 eV/O, and -0.5 eV/O for C_1O, C_2O, and C_4O, respectively. We can clearly see that C_1O has the lowest formation energy and the formation energy increases with the decrease of the oxygen concentration. We note that the above results are based

on the GA simulations with finite supercell size. We now discuss the possible structure of oxidized graphene with an infinite large graphene supercell. The two low energy structures of C_1O should remain the same because of the perfect ordering and low formation energy. For oxidized graphene with less oxygen atoms than carbon atoms, the phase separation between the C_1O phase and bare graphene will occur. The phase separation is caused by the tendency to minimize the number of broken carbon-carbon π-π bonds, as in the case of partially hydrogenated graphene [29]. The tendency toward phase separation is manifested in the lowest energy structure of C_2O [Fig. 2(a)] and is confirmed in the case of C_4O: If we double the cell of Fig. 2(d) along the direction perpendicular to the isolated epoxy pair chain and move the two epoxy pair chains close to each other, the resulting C_4O structure will have a formation energy of -0.87 eV/O. In contrast, increasing the cell of Fig. 2(c) does not lead to a significant decrease of the formation energy.

Our calculations indicate that the two low energy phases of C_1O will probably exist in any oxidized graphene. Therefore, the electronic properties of the C_1O phases is of paramount importance. Because the LDA is well known to underestimate the band gaps of semiconductors, we calculate the band structure of the C_1O phases by employing the screened Heyd-Scuseria-Ernzerhof 06 (HSE06) hybrid functional [30], which was shown to give a good band gap for many semiconductors including graphene based systems [31]. Our calculations show that the C_1O phase with the mix model is a semiconductor with a large band gap of 5.90 eV [Fig. 3(a)]. The valence band maximum (VBM) locates at Γ, but the CBM is almost non-dispersive, which is consistent with the fact that the CBM state at Γ is an antibonding C-O orbital mostly localized in the six-membered carbon rings [see the inset of Fig. 3(a)]. Fig. 3(b) shows that the C_1O phase with the epoxy pair model is also a semiconductor but with a smaller indirect band gap of 2.14 eV. The VBM and CBM locate at (0.5, 0, 0) and Γ, respectively. An important difference between the two phases is that the C_1O phase with the epoxy pair model has a much smaller electron and hole effective mass. This is because the band overlap is stronger in the epoxy pair model with a higher symmetry, as can be seen from the CBM wavefunction displayed in the inset of Fig. 3(b). The larger band gap and lower energy in the mix model is a consequence of its lower symmetry (C_{2v}): Level repulsions between the occupied and unoccupied bands which are symmetrically forbidden in the epoxy pair model (D_{2h}) become possible in the mix model.

We also calculate the absolute values of the VBM and CBM levels using the HSE06 hybrid functional, which was found [32, 33] to give improved results compared to the LDA functional. The vacuum level is defined as the average electrostatic potential in the vacuum region where it approaches a constant [32]. For comparison, we also calculate the work function of graphene. Our results are shown in Fig. 3(c). As expected, the VBM of both C_1O phases are below the Fermi level of graphene due to the oxygen $2p$ orbitals with low energies. And the CBM level of the C_1O phase with the mix model is higher than the Fermi level of graphene by 1.6 eV. Interestingly and surprisingly, the CBM level of the C_1O phase with the epoxy pair model is lower than the Dirac point of graphene. This is because the low oxygen 2s and 2p orbitals and the formation of one dimensional zizag chain by carbon $2p_z$ orbitals dramatically lowers the eigenvalue of the CBM state [see the inset of Fig. 3(b)]. It is noted that LDA gives qualitatively similar band alignment. This will have interesting consequences as will be discussed below.

The experimentally synthesized graphene oxide usually has a much lower oxygen concentration than the C_1O phases. Here, we will discuss the electronic structures of partially oxidized graphene. As shown above, there is a phase separation between the graphene part and the C_1O phase in the partially oxidized graphene under thermodynamic equilibrium. The C_1O phase with the epoxy pair model could match graphene well via a zigzag-like edge with a lattice mismatch of 6.0 % [Fig. 4(b)]. However, the lattice mismatch between the C_1O phase with the mix model and graphene is much larger: The smallest mismatch (21.9%) occurs when the C_1O phase connects with graphene via an armchair edge [Fig. 4(a)]. As expected, there is a band gap openning [See Fig. 4(c)] in the partially oxidized graphene with a phase separation between graphene and the C_1O phase with the mix model. This is due to quantum confinement effect, similar to the armchair graphene nanoribbon case [34]. In contrast, the partially oxidized graphene with a zigzag-like edge between graphene and the C_1O phase with the epoxy pair model is metallic [See Fig. 4(d)]. And there is no flat band and inclusion of spin degree of freedom does not open a gap, different from the zigzag graphene nanoribbon case [34]. The metallicity of the system is not due to the peculiar zigzag-like interface between graphene and the C_1O phase because a test calculation on a system similar to that shown in Fig. 4(a) but with an armchair interface between graphene and the C_1O phase with the epoxy pair model is also metallic. This is due to the fact that the CBM of the C_1O phase with the epoxy pair model is lower than graphene, thus there is

almost no quantum confinement effect and no flat edge states.

In summary, we have performed global search of the lowest energy structures of oxidized graphene using the genetic algorithm approach combined with density functional theory. Our calculations unravel two novel low energy semiconducting phases of fully oxidized graphene C_1O. The C_1O phase with the epoxy pair model has an indirect band gap of about 2.14 eV, and an extremely low CBM that is below the Fermi level of graphene. The ground state of the C_1O phase with three mixed epoxy groups has a lower energy by only 60 meV/O than the C_1O phase within the epoxy pair model and a much larger band gap. Our calculations predict that the phase separation between bare graphene and fully oxidized graphene is thermodynamically favorable in partially oxidized graphene. The C_1O phase with the epoxy pair model has a much smaller lattice mismatch with graphene than the case of the mix model. In the partially oxidized graphene with a zigzag-like edge between graphene and the C_1O phase with the epoxy pair model, there is no band gap openning and no local spin moment as a result of the unusually low CBM of the C_1O phase.

Work at Fudan was supported by the National Science Foundation of China. Work at NREL was supported by the U.S. Department of Energy, under Contract No. DE-AC36-08GO28308. We thank Dr. Gus Hart for useful discussion at the early stage on this project.

[1] K. S. Novoselov, A. K. Geim, S. V. Morozov, D. Jiang, M. I. Katsnelson, I. V. Grigorieva, S. V. Dubonos, and A. A. Firsov, Nature (London) **438**, 197 (2005).

[2] K. S. Novoselov, E. McCann, S. V. Morozov, V. I. Falko, M. I. Katsnelson, U. Zeitler, D. Jiang, F. Schedin, and A. K. Geim, Nat. Phys. **2**, 177 (2006).

[3] Y. B. Zhang, Y. W. Tan, H. L. Stormer, P. Kim, Nature (London) **438**, 201 (2005).

[4] M. I. Katsnelson, K. S. Novoselov, A. K. Geim, Nat. Phys. **2**, 620 (2006).

[5] F. Miao, S. Wijeratne, Y. Zhang, U. C. Coskun, W. Bao, and C. N. Lau, Science **317**, 1530 (2007).

[6] A. K. Geim and K. S. Novoselov, Nat. Mater. **6**, 183 (2007).

[7] C. Gómez-Navarro, R. T. Weitz, A. M. Bittner, M. Scolari, A. Mews, M. Burghard, and K. Kern, Nano Lett. **7**, 3499 (2007).

[8] G. Eda, G. Fanchini, and M. Chhowalla, Nat. Nanotech. **3**, 270 (2008).

[9] V. C. Tung, M. J. Allen, Y. Yang, and R. B. Kaner, Nat. Nanotech. **4**, 25 (2009).

[10] D. Li, M. B. Muller, S. Gilje, R. B. Kaner, and G. G. Wallace, Nat. Nanotech. **3**, 101 (2008).

[11] S. Gijie, S. Han, M. Wang, K. L. Wang, and R. B. Kaner, Nano Lett. **7**, 3394 (2007).

[12] S. Stankovich, D. A. Dikin, G. H. B. Dommett, K. M. Kohlhaas, E. J. Zimney, E. A. Stach, R. D. Piner, S. T. Nguyen, and R. S. Ruoff, Nature (London) **442**, 282 (2006).

[13] B. Brodie, Phil. Trans. **149**, 249 (1859).

[14] N. R. Wilson, P. A. Pandey, R. Beanland, R. J. Young, I. A. Kinloch, L. Gong, Z. Liu, K. Suenaga, J. P. Rourke, S. J. York, and J. Sloan, ACS Nano, **3**, 2547 (2009).

[15] W. Gao, L. B. Alemany, L. Ci, and P. M. Ajayan, Nat. Chem. **1**, 403 (2009).

[16] W. W. Cai, R. D. Piner, F. J. Stadermann, S. Park, M. A. Shaibat, Y. Ishii, D. X. Yang, A. Velamakanni, S. J. An, M. Stoller, J. H. An, D. M. Chen, and R. S. Ruoff, Science **321**, 1815 (2008).

[17] K. N. Kudin, B. Ozbas, H. C. Schniepp, R. K. Prud'homme, I. A. Aksay, and R. Car, Nano Lett. **8**, 36 (2008).

[18] D.W. Boukhvalov and M. I. Katsnelson, J. Am. Chem. Soc. **130**, 10697 (2008).

[19] J.-A. Yan, L. Xian, and M. Y. Chou, Phys. Rev. Lett. **103**, 086802 (2009).

[20] R. J. W. E. Lahaye, H. K. Jeong, C. Y. Park, and Y. H. Lee, Phys. Rev. B **79**, 125435 (2009)

[21] L. Liu, S. Ryu, M. R. Tomasik, E. Stolyarova, N. Jung, M. S. Hybertsen, M. L. Steigerwald, L. E. Brus, and G. W. Flynn, Nano Lett. **8**, 1965 (2008).

[22] D. C. Kim, D.-Y. Jeon, H.-J. Chung, Y. Woo, J. K. Shin, and S. Seo, Nanotechnology **20**, 375703 (2009).

[23] D. M. Deaven and K. M. Ho, Phys. Rev. Lett. **75**, 288 (1995)

[24] J. Z. Liu, G. Trimarchi, and A. Zunger, Phys. Rev. Lett. **99**, 145501 (2007).

[25] A. R. Oganov and C.W. Glass, J. Chem. Phys. **124**, 244704 (2006).

[26] P. E. Blöchl, Phys. Rev. B **50**, 17953 (1994); G. Kresse and D. Joubert, *ibid* **59**, 1758 (1999).

[27] G. Kresse and J. Furthmüller, Comput. Mater. Sci. **6**, 15 (1996); Phys. Rev. B **54**, 11169 (1996);

[28] Z. Y. Li, W. H. Zhang, Y. Luo, J. L. Yang and J. G. Hou, J. Am. Chem. Soc. **131**, 6320 (2009).

[29] H. J. Xiang, E. J. Kan, S.-H. Wei, M.-H. Whangbo, and J. L. Yang, Nano Lett. **9**, 4025 (2009).

[30] J. Heyd, G. E. Scuseria, and M. Ernzerhof, J. Chem. Phys. **118**, 8207 (2003).

[31] O. Hod, V. Barone, and G. E. Scuseria, Phys. Rev. B **77**, 035411 (2008).

[32] H. J. Xiang, and S.-H. Wei, and X. G. Gong, J. Phys. Chem. C **113**, 18968 (2009).

[33] A. Alkauskas, P. Broqvist, F. Devynck, and A. Pasquarello, Phys. Rev. Lett. **101**, 106802 (2008).

[34] L. Yang, C.-H. Park, Y.-W. Son, M. L. Cohen, and S. G. Louie, Phys. Rev. Lett. **99**, 186801 (2007).

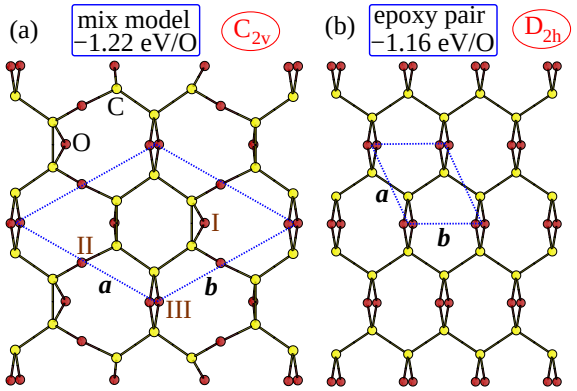

FIG. 1: (Color online) (a) The structure of the mix model (C_{2v} symmetry) which is predicted to be the lowest energy C_1O phase. (b) The low energy C_1O phase with the epoxy pair model (D_{2h} symmetry), which has a higher energy by only 0.06 eV/O than the mix model. "I", "II", and "III" in (a) indicate normal epoxy, unzipped epoxy, and epoxy pair, respectively. The unit cells are enclosed by dashed lines. The numbers give the formation energy of the oxidized graphene structures.

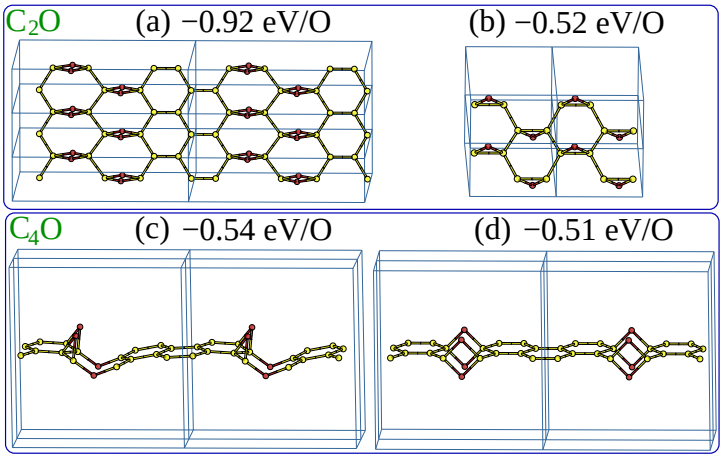

FIG. 2: (Color online) (a) shows the newly predicted lowest energy structure of the C_2O phase among all configurations with no more than eight carbon atoms per cell. (b) is the model of the C_2O phase predicted by Yan *et al.* [19]. (c) shows the lowest energy structure of the C_4O phase among all configurations with no more than eight carbon atoms per cell. (d) is a low energy structure of the C_4O phase which has a higher energy by only 0.03 eV/O than the lowest energy structure.

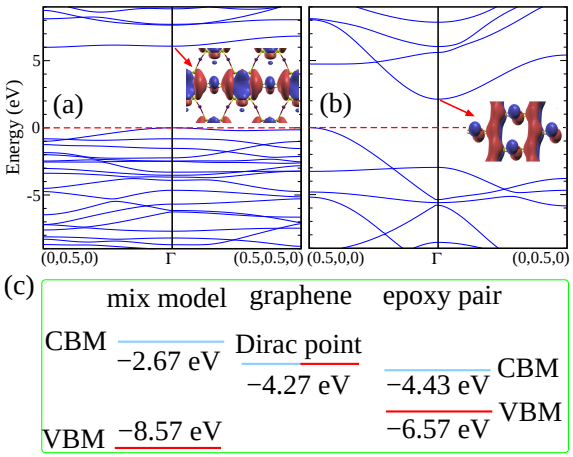

FIG. 3: (Color online) (a) and (b) show the band structures from the hybrid HSE06 calculations of the C_1O phases with the mix model and epoxy pair model, respectively. In the insets, we show the wavefunction plots of the LUMO states at Γ. The k-points are given in terms of the reciprocal lattice. (c) Schematic illustration of the band alignment between the two C_1O phases and graphene from the hybrid HSE06 calculations.

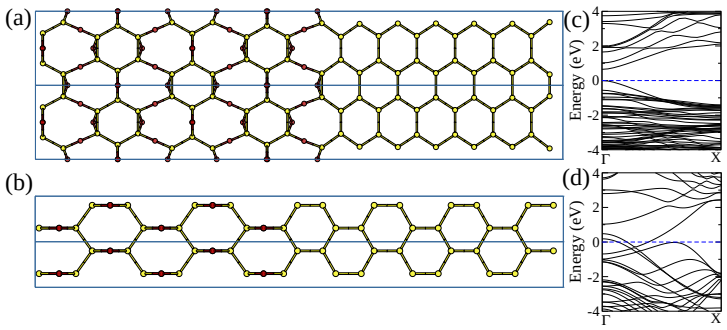

FIG. 4: (Color online) (a) shows a partially oxidized graphene with an armchair edge between bare graphene and the C_1O phase with the mix model. (b) displays a partially oxidized graphene with a zigzag-like edge between bare graphene and the C_1O phase with the epoxy pair model. (c) and (d) show the corresponding LDA band structures.